

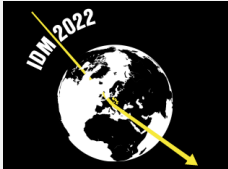
Search for low mass WIMP dark matter with DarkSide-50

Masato Kimura^{1*} on behalf of DarkSide-50 Collaboration

1 AstroCeNT, Nicolaus Copernicus Astronomical Center, 00-614 Warsaw, Poland

* mkimura@camk.edu.pl

October 3, 2022



14th International Conference on Identification of Dark Matter

Vienna, Austria, 18-22 July 2022

doi:[10.21468/SciPostPhysProc.7](https://doi.org/10.21468/SciPostPhysProc.7)

Abstract

DarkSide-50 is a direct dark matter detection experiment at Laboratori Nazionali del Gran Sasso that uses argon as the target material. Exploiting the ionization signal from a dual-phase time projection chamber filled with low-radioactivity argon, it has set the most stringent exclusion limit on WIMPs with a mass of few GeV/c^2 . A new analysis has recently been carried out with a larger exposure, profiting from an improved understanding of the detector response and background model. An improvement of about a factor 10 in sensitivity is expected for a WIMP mass of $2 \text{ GeV}/c^2$.

1 Introduction

Dark matter direct detection experiments search for a signal induced by an interaction between the dark matter particle candidate and Standard Model particles. The primary goal of the DarkSide program is to detect dark matter in the form of Weakly Interacting Massive Particles (WIMPs) scattering off an argon nucleus, using a dual-phase time projection chamber (TPC). For WIMP masses higher than $10 \text{ GeV}/c^2$, signal is discriminated from background by means of an accurate topological reconstruction which relies both on scintillation (S1) and ionization (S2) signals [1]. For lower masses, on the other hand, the scintillation signal is no longer observable and an excess of event is sought above the background expectation using the ionization-signal-only (S2-only analysis). The world-class sensitivity is achievable by this approach owing to the relatively low atomic mass of argon, to the intrinsically low background rate of the detector, and to the almost 100% efficiency of the single electron detection.

The DarkSide program foresees a multi-stage approach. A 50 kg-scale detector, DarkSide-50 (DS-50), was operated between 2013 and 2019 at Laboratori Nazionali del Gran Sasso (LNGS), and the first result of the low-mass WIMP search was published in 2018 [2]. Since then, we reanalyzed data both from calibration campaigns [3] and the WIMP search run with increasing exposure. In this work, we present in detail new analysis for the WIMP search.

2 DarkSide-50

The DS-50 TPC has a cylindrical active mass of $(46.4 \pm 0.7) \text{ kg}$ filled with low-radioactivity argon extracted from deep underground sources [4]. Ionization electrons from an energy

deposition inside the active region drift towards the liquid-gas interface at the top of the TPC by the applied electric field of 200 V/cm. The electrons are then extracted to the gas phase by a higher electric field (2.8 kV/cm in the liquid and 4.2 kV/cm in the gas phases) where they emit electroluminescence light (S2). Photomultiplier tubes (PMTs) located on both ends of the TPC detect the S2 light. The electron extraction efficiency is estimated to be higher than 99.9% and the observed S2 amplification gain at the center of the TPC is (23 ± 1) photoelectrons/ e^- .

3 Event selection

The dataset used in this work corresponds to a total live time of 653.1 days from December 2015 to February 2018. Volume fiducialization is performed based on the position of the top-array PMT which measures the largest fraction of S2 photons, as was done in the previous analysis, to suppress the exposure to external radioactive contamination. The fiducial volume, which corresponds to 41.9% of the total argon active volume, is defined by suppressing events reconstructed near the walls of the TPC. The resulting total exposure, including the selection cuts described below, is (12306 ± 184) kg d, about 1.8 times larger than the previous analysis.

Further selections are applied to remove S2 pulses incompatible with the signal hypothesis. Pulses composed by several S1 and/or S2 pulses but mis-reconstructed to be one pulse are rejected by pulse shape parameters, such as the fraction of light observed in the first 90 ns (f_{90}), the pulse peak time relative to its start time, and its FWHM. Signal acceptance of these selections is evaluated to be higher than 95% via Monte Carlo (MC) simulation.

Another selection criterion requires that the previous event has triggered the DAQ more than 20 ms before any triggered event. This requirement removes the so-called spurious electron events, whose origin is likely due to ionization electrons trapped along their drift by impurities and released with some delay. The 20 ms veto reduces the total livetime by 3%.

An S2 pulse following an anomalously large S1 pulse is also rejected, where the S1 pulse is distinguished by f_{90} . The origin of these events is found to be due to α decays on the surfaces or shallow depth of the TPC walls; the ionization electrons associated with the S1 are absorbed by the wall before reaching the gas phase but the scintillation photons can extract other electrons from the cathode by photoelectric effect. The cut line in the two dimension space of the S1 versus S2/S1 ratio is derived from ^{39}Ar and ^{241}Am - ^7Be calibration campaigns and defined in order to contain 99% of the signal.

Fig. 1 shows the electron spectra at different steps of the event selection. The final sample consists of the S1-plus-S2 and S2-only (without a corresponding S1 pulse) subsamples, as shown by the blue and orange shaded histograms, respectively.

4 Background modeling

The majority of events in the region of interest (RoI) comes from either β -rays from diffused isotopes in liquid argon (^{85}Kr and ^{39}Ar) or γ -rays from detector components.

The specific activities of ^{85}Kr and ^{39}Ar are assessed by fitting the energy spectrum far above the RoI taken before the current dataset. The ^{85}Kr activity is also estimated by counting the number of $\beta + \gamma$ fast-coincidence events which is due to one of the ^{85}Kr decay scheme with the branching ratio of 0.43% (the lifetime between the β - and γ -decays is $1.46 \mu\text{s}$). The spectrum shapes of ^{85}Kr and ^{39}Ar are also updated from the previous analysis by taking into account recent calculations of atomic exchange and screening effects [5, 6] with uncertainties as shown in Fig. 2 (left).

The event rate from the γ -rays from detector materials is evaluated using an extensive MC

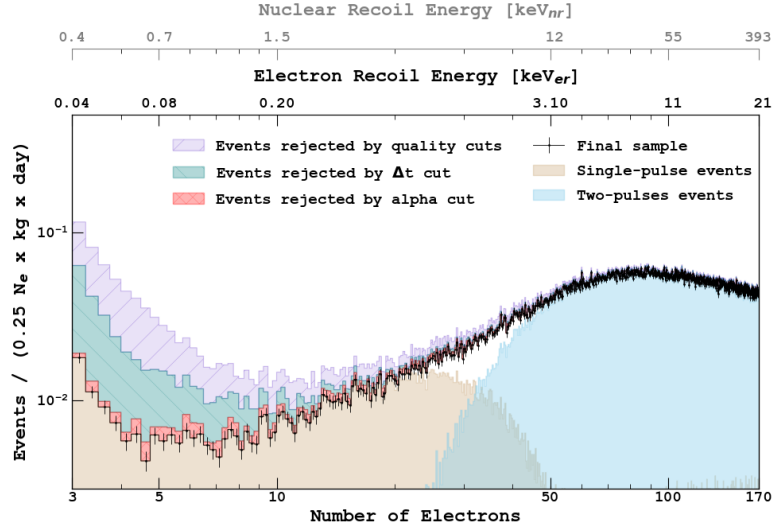


Figure 1: Observed electron spectra at different steps of the event selection.

simulation based on material radio-assay result, unlike the previous analysis in which they were extrapolated from a fit to the higher energy region. Two main sources of this type of background are found to be due to residual activity in the PMTs and stainless-steel cryostat, as shown in Fig. 2 (right). Expected spectra from these sources are incorporated in this analysis with associated uncertainties.

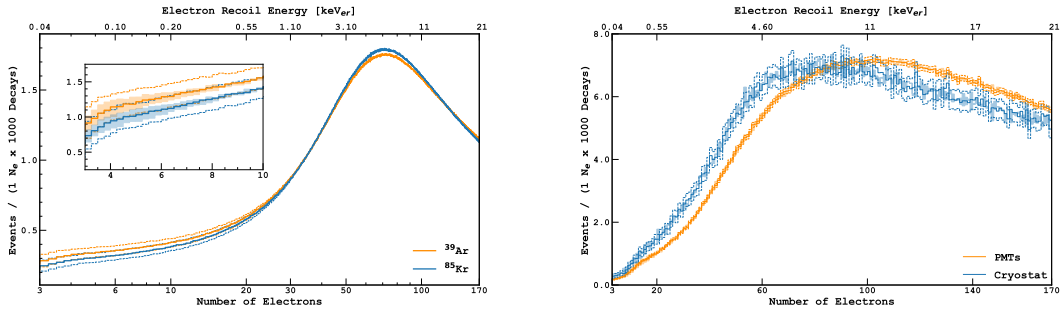


Figure 2: Internal (left) and external (right) background spectra used in this analysis. The dashed line represents the uncertainty from the detector response model. The shaded region of the internal background corresponds to the uncertainty from the spectrum shape calculation, while that of the external background comes from the statistics of the MC.

5 Result

The WIMP sensitivity is determined based on the binned ionization spectrum using a test-statistics based on the profile-likelihood-ratio [7]. Systematic uncertainties included in this analysis cover the uncertainty in the determination of the fiducial volume (1.5%), the uncertainty on the activities of each background component (4.7%–14.0%), uncertainties on β -decay spectrum calculation, and on the determination of the ionization yields. The new ionization yield calibration with its uncertainty has been validated up to 22 keV_{er}. This allows

us to expand the number of electron (N_e) RoI in this analysis to $N_e = [4, 170]$, compared with $N_e = [4, 50]$ in the previous one.

As we are not aware of any data constraining the fluctuation of the ionization yield for NR in the energy range of interest, we keep the strategy from the previous analysis to consider two extreme cases for the fluctuation, with (QF) and without (NQ) quenching fluctuations. Fig. 3 shows the expected sensitivities for both cases.

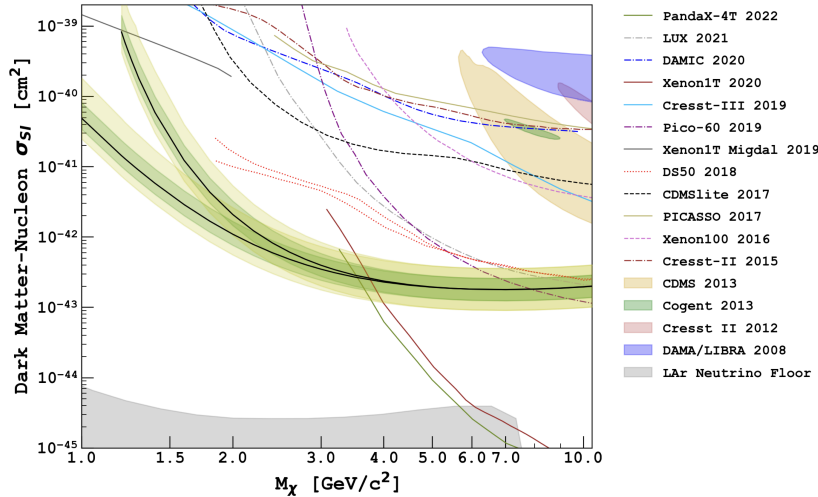


Figure 3: Expected limits for NQ (upper black solid line) and QF (lower line) models, together with the $\pm 1\sigma$ (green) and $\pm 2\sigma$ (yellow) bands. Also shown are the 90% C.L. exclusion limits and claimed discovery from various other experiments [2, 8–20] and the neutrino floor for argon experiments [21].

6 Conclusion

A new search for low mass WIMP dark matter has been conducted using the low radioactivity argon campaign of the DS-50. Compared to the previous one published in 2018, this new analysis benefits from many updates such as (1) the larger exposure, (2) improved event selection criteria based on better understanding of detector response, (3) more accurate background modeling, (4) more precise calibration of the ionization yields for both NR and ER, and (5) expanded threshold. About a factor 10 improved sensitivity is expected around the WIMP mass of a few GeV/c^2 region.

The final results with the observed limits are discussed in detail in Ref. [22].

Acknowledgements

The DarkSide Collaboration offers its profound gratitude to the LNGS and its staff for their invaluable technical and logistical support. We also thank the Fermilab Particle Physics, Scientific, and Core Computing Divisions. Construction and operation of the DarkSide-50 detector was supported by the U.S. National Science Foundation (NSF) (Grants No. PHY-0919363, No. PHY-1004072, No. PHY-1004054, No. PHY-1242585, No. PHY-1314483, No. PHY-1314501, No. PHY-1314507, No. PHY-1352795, No. PHY-1622415, and associated collaborative grants No. PHY-1211308 and No. PHY-1455351), the Italian Istituto Nazionale di Fisica Nucleare, the

U.S. Department of Energy (Contracts No. DE-FG02-91ER40671, No. DEAC02-07CH11359, and No. DE-AC05-76RL01830), the Polish NCN (Grant No. UMO-2014/15/B/ST2/02561) and the Foundation for Polish Science (Grant No. Team2016-2/17). We also acknowledge financial support from the French Institut National de Physique Nucléaire et de Physique des Particules (IN2P3), the IN2P3-COPIN consortium (Grant No. 20-152), and the UnivEarthS LabEx program (Grants No. ANR-10-LABX-0023 and No. ANR-18-IDEX-0001), from the São Paulo Research Foundation (FAPESP) (Grant No. 2016/09084-0), from the Interdisciplinary Scientific and Educational School of Moscow University “Fundamental and Applied Space Research”, from the Program of the Ministry of Education and Science of the Russian Federation for higher education establishments, project No. FZWG-2020-0032 (2019-1569), from IRAP AstroCeNT funded by FNP from ERDF, and from the Science and Technology Facilities Council, United Kingdom. The theoretical calculation of beta decays was performed as part of the EMPIR Project 20FUN04 PrimA-LTD. This project has received funding from the EMPIR program co-financed by the Participating States and from the European Union’s Horizon 2020 research and innovation program. Furthermore, this project has received funding from the European Union’s Horizon 2020 research and innovation program under grant agreement No 952480. Isotopes used in this research were supplied by the United States Department of Energy Office of Science by the Isotope Program in the Office of Nuclear Physics.

References

- [1] P. Agnes *et al.*, *DarkSide-50 532-day Dark Matter Search with Low-Radioactivity Argon*, Phys. Rev. D **98**(10), 102006 (2018), doi:[10.1103/PhysRevD.98.102006](https://doi.org/10.1103/PhysRevD.98.102006), [1802.07198](https://arxiv.org/abs/1802.07198).
- [2] P. Agnes *et al.*, *Low-Mass Dark Matter Search with the DarkSide-50 Experiment*, Phys. Rev. Lett. **121**(8), 081307 (2018), doi:[10.1103/PhysRevLett.121.081307](https://doi.org/10.1103/PhysRevLett.121.081307), [1802.06994](https://arxiv.org/abs/1802.06994).
- [3] P. Agnes *et al.*, *Calibration of the liquid argon ionization response to low energy electronic and nuclear recoils with DarkSide-50*, Phys. Rev. D **104**(8), 082005 (2021), doi:[10.1103/PhysRevD.104.082005](https://doi.org/10.1103/PhysRevD.104.082005), [2107.08087](https://arxiv.org/abs/2107.08087).
- [4] P. Agnes *et al.*, *Results From the First Use of Low Radioactivity Argon in a Dark Matter Search*, Phys. Rev. D **93**(8), 081101 (2016), doi:[10.1103/PhysRevD.93.081101](https://doi.org/10.1103/PhysRevD.93.081101), [Addendum: Phys.Rev.D 95, 069901 (2017)], [1510.00702](https://arxiv.org/abs/1510.00702).
- [5] X. Mougeot and C. Bisch, *Consistent calculation of the screening and exchange effects in allowed β^- transitions*, Phys. Rev. A **90**, 012501 (2014), doi:[10.1103/PhysRevA.90.012501](https://doi.org/10.1103/PhysRevA.90.012501).
- [6] S. J. Haselschwardt, J. Kostensalo, X. Mougeot and J. Suhonen, *Improved calculations of beta decay backgrounds to new physics in liquid xenon detectors*, Phys. Rev. C **102**, 065501 (2020), doi:[10.1103/PhysRevC.102.065501](https://doi.org/10.1103/PhysRevC.102.065501), [2007.13686](https://arxiv.org/abs/2007.13686).
- [7] G. Cowan, K. Cranmer, E. Gross and O. Vitells, *Asymptotic formulae for likelihood-based tests of new physics*, Eur. Phys. J. C **71**, 1554 (2011), doi:[10.1140/epjc/s10052-011-1554-0](https://doi.org/10.1140/epjc/s10052-011-1554-0), [Erratum: Eur.Phys.J.C 73, 2501 (2013)], [1007.1727](https://arxiv.org/abs/1007.1727).
- [8] W. Ma *et al.*, *A First Search for Solar ^8B Neutrino in the PandaX-4T Experiment using Neutrino-Nucleus Coherent Scattering* (2022), [2207.04883](https://arxiv.org/abs/2207.04883).
- [9] M. Traina *et al.*, *Results on low-mass weakly interacting massive particles from a 11 kg d target exposure of DAMIC at SNOLAB*, PoS **ICRC2021**, 539 (2021), doi:[10.22323/1.395.0539](https://doi.org/10.22323/1.395.0539), [2108.05983](https://arxiv.org/abs/2108.05983).

- [10] A. H. Abdelhameed *et al.*, *First results from the CRESST-III low-mass dark matter program*, Phys. Rev. D **100**(10), 102002 (2019), doi:[10.1103/PhysRevD.100.102002](https://doi.org/10.1103/PhysRevD.100.102002), [1904.00498](https://arxiv.org/abs/1904.00498).
- [11] G. Angloher *et al.*, *Results from 730 kg days of the CRESST-II Dark Matter Search*, Eur. Phys. J. C **72**, 1971 (2012), doi:[10.1140/epjc/s10052-012-1971-8](https://doi.org/10.1140/epjc/s10052-012-1971-8), [1109.0702](https://arxiv.org/abs/1109.0702).
- [12] C. Amole *et al.*, *Dark Matter Search Results from the PICO-60 C₃F₈ Bubble Chamber*, Phys. Rev. Lett. **118**(25), 251301 (2017), doi:[10.1103/PhysRevLett.118.251301](https://doi.org/10.1103/PhysRevLett.118.251301), [1702.07666](https://arxiv.org/abs/1702.07666).
- [13] E. Aprile *et al.*, *Search for inelastic scattering of WIMP dark matter in XENON1T*, Phys. Rev. D **103**(6), 063028 (2021), doi:[10.1103/PhysRevD.103.063028](https://doi.org/10.1103/PhysRevD.103.063028), [2011.10431](https://arxiv.org/abs/2011.10431).
- [14] E. Aprile *et al.*, *Search for Light Dark Matter Interactions Enhanced by the Migdal Effect or Bremsstrahlung in XENON1T*, Phys. Rev. Lett. **123**(24), 241803 (2019), doi:[10.1103/PhysRevLett.123.241803](https://doi.org/10.1103/PhysRevLett.123.241803), [1907.12771](https://arxiv.org/abs/1907.12771).
- [15] R. Agnese *et al.*, *Low-mass dark matter search with CDMSlite*, Phys. Rev. D **97**(2), 022002 (2018), doi:[10.1103/PhysRevD.97.022002](https://doi.org/10.1103/PhysRevD.97.022002), [1707.01632](https://arxiv.org/abs/1707.01632).
- [16] R. Agnese *et al.*, *Search for Low-Mass Weakly Interacting Massive Particles Using Voltage-Assisted Calorimetric Ionization Detection in the SuperCDMS Experiment*, Phys. Rev. Lett. **112**(4), 041302 (2014), doi:[10.1103/PhysRevLett.112.041302](https://doi.org/10.1103/PhysRevLett.112.041302), [1309.3259](https://arxiv.org/abs/1309.3259).
- [17] D. S. Akerib *et al.*, *Improving sensitivity to low-mass dark matter in LUX using a novel electrode background mitigation technique*, Phys. Rev. D **104**(1), 012011 (2021), doi:[10.1103/PhysRevD.104.012011](https://doi.org/10.1103/PhysRevD.104.012011), [2011.09602](https://arxiv.org/abs/2011.09602).
- [18] E. Behnke *et al.*, *Final Results of the PICASSO Dark Matter Search Experiment*, Astropart. Phys. **90**, 85 (2017), doi:[10.1016/j.astropartphys.2017.02.005](https://doi.org/10.1016/j.astropartphys.2017.02.005), [1611.01499](https://arxiv.org/abs/1611.01499).
- [19] C. E. Aalseth *et al.*, *Results from a Search for Light-Mass Dark Matter with a P-type Point Contact Germanium Detector*, Phys. Rev. Lett. **106**, 131301 (2011), doi:[10.1103/PhysRevLett.106.131301](https://doi.org/10.1103/PhysRevLett.106.131301), [1002.4703](https://arxiv.org/abs/1002.4703).
- [20] R. Bernabei *et al.*, *Final model independent result of DAMA/LIBRA-phase1*, Eur. Phys. J. C **73**, 2648 (2013), doi:[10.1140/epjc/s10052-013-2648-7](https://doi.org/10.1140/epjc/s10052-013-2648-7), [1308.5109](https://arxiv.org/abs/1308.5109).
- [21] F. Ruppin, J. Billard, E. Figueroa-Feliciano and L. Strigari, *Complementarity of dark matter detectors in light of the neutrino background*, Phys. Rev. D **90**(8), 083510 (2014), doi:[10.1103/PhysRevD.90.083510](https://doi.org/10.1103/PhysRevD.90.083510), [1408.3581](https://arxiv.org/abs/1408.3581).
- [22] P. Agnes *et al.*, *Search for low-mass dark matter WIMPs with 12 ton-day exposure of DarkSide-50* (2022), [2207.11966](https://arxiv.org/abs/2207.11966).